Journal of ELECTRONIC MATERIALS, Vol. 44, No. 6, 2015
DOI: 10.1007/s11664-014-3579-2

Optimization of Cooling Unit Design for Automotive Exhaust-Based Thermoelectric Generators

C.Q. SU,[1,2] M. XU,[1] W.S. WANG,[1] Y.D. DENG,[1] X. LIU,[1] and Z.B. TANG[1]

1.—Hubei Key Laboratory of Advanced Technology for Automotive Components, Automobile Engineering Institute, Wuhan University of Technology, 205 Luoshi Road, Hongshan District, Wuhan 430070, China. 2.—e-mail: suchuqi@whut.edu.cn

Integrating a thermoelectric cooler (TEC) into the engine cooling system has various advantages including reducing additional mechanical parts, and saving energy and space for automotive applications. Based on performance parameters of the engine and thermoelectric modules, three different TEC configurations called plate-shape, stripe-shape, and diamond-shape are constructed with development of simulations of the different TECs and the performance of the circulating coolant. Based on these simulations, the velocity, pressure, and temperature fields of the coolant are obtained for further research. Besides, the temperature of the TEC and the output power of the thermoelectric generator (TEG) are acquired experimentally. Comparing the working performance of the different TECs, the simulation and experimental results show that the TEG using the diamond-shaped TEC achieves a relatively ideal performance. Finally, some measures are proposed to improve the cooling system, providing guidelines for future research.

Key words: Automotive exhaust heat, TEG, TEC, cooling performance

INTRODUCTION

Currently, approximately 40% of the fuel energy is lost via the exhaust, intensifying the energy crisis and environmental pollution.[1] As vehicle exhaust emission regulations become increasingly harsh, new technologies have been developed to control emissions and improve the efficiency of waste heat recovery. Thermoelectric generation technology may offer thermoelectric energy conversion with advantages of being highly reliable, zero emission, low noise, and involving no moving parts. Due to these merits, application of thermoelectric generation technology in automobiles must be discussed. Hsiao and Chang[2] constructed a mathematic model to predict the performance of thermoelectric modules (TEMs) attached to a waste heat recovery system, showing that TEMs can offer better performance on the exhaust pipe than on the radiator. Rezania and Rosendahl[3] applied a microchannel heat sink to explore the effective pumping power required for thermoelectric generators (TEGs). Some research into the compatibility of the thermoelectric cooler (TEC) and engine cooling system were carried out by Deng,[4] who found that the coolant temperature would exceed the boiling point at high engine power and low vehicle speed when the TEC was inserted into the engine cooling system. According to the fundamental formula of the Seebeck effect in Eq. 1,

$$\Delta V = N \cdot \alpha_{pn} \cdot (T_{\mathrm{h}} - T_{\mathrm{c}}), \tag{1}$$

where α_{pn} is the relative thermoelectric Seebeck coefficient, i.e., the difference between α_p and α_n, N is the number of TEMs, and T_{h} and T_{c} are the temperatures of the heat exchanger and the TEC, it can be noticed that the open-circuit voltage of the TEM mainly depends on the temperature difference between the cold and hot sides of the module. Therefore, apart from optimization of the heat exchanger and the thermoelectric materials, design and optimization of the TEC is also an effective way to promote overall TEG efficiency.

(Received July 3, 2014; accepted December 3, 2014; published online January 7, 2015)

In this case study, an entire TEG system for recovering automotive waste heat was built. As well as some computational simulations, corresponding bench tests were also carried out to validate the simulation models. On the basis of the simulation and experimental results, the performance of different TECs was analyzed to determine the most appropriate one to enhance the overall performance of the TEG system, as presented below.

GEOMETRY AND SIMULATION SETUP

Geometric Model

Computational fluid dynamics (CFD) was used to simulate the coolant flow within different TECs, obtaining the temperature distribution, velocity field, and pressure field.[5] To simplify the modeling complexity, various hypothetical conditions were applied as follows:

1. Thermal and flow effects are in the steady state, and no phase changes occur inside the TEC.
2. The coolant is regarded as an incompressible Newtonian fluid.
3. Heat conduction is perpendicular to the flow direction; both heat conduction in the axial direction and heat radiation are omitted.

TEMs made of semiconductor materials were sandwiched between the heat exchanger and the TEC in an exhaust-based TEG. This sandwich structure is maintained by clamping devices, and the whole structure is shown in Fig. 1. In the process of heat transfer from the heat source and release into the coolant flow, part of the heat is converted into electrical energy in the form of output power or electromotive force. According to previous study on the thermal optimization of a heat exchanger for automotive exhaust-based TEGs, the external dimensions of the rectangular heat exchanger were determined to be 660 mm long by 305 mm wide in order to achieve a more uniform temperature distribution and higher interface temperature. Considering the number of TEMs and the outer size of the heat exchanger, three different TEC configurations called plate-shape, stripe-shape, and diamond-shape were constructed. The different structures of the whole TEG system using the plate-shaped, stripe-shaped, and diamond-shaped TEC are presented in Fig. 2. It can be seen that the TEC is fixed by a clamping mechanism composing the cold side of the TEG system. Among

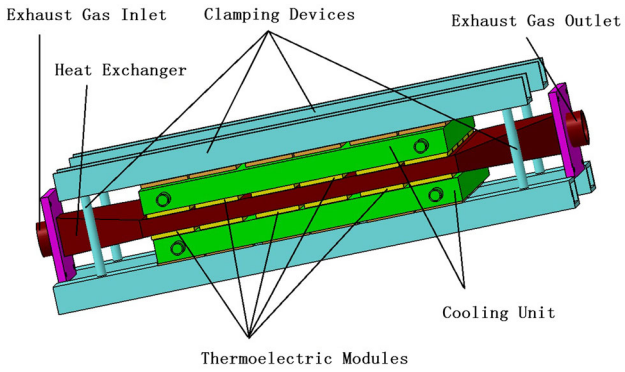

Fig. 1. Schematic diagram of TEG system.

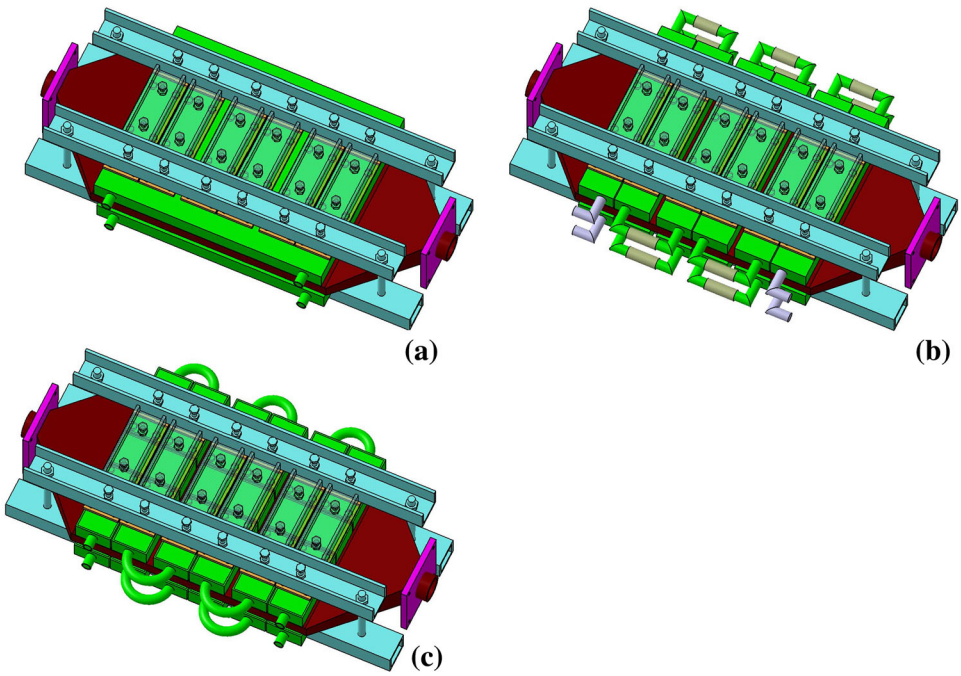

Fig. 2. Three-dimensional model of TEG system using plate-shaped (a), stripe-shaped (b), and diamond-shaped (c) TEC.

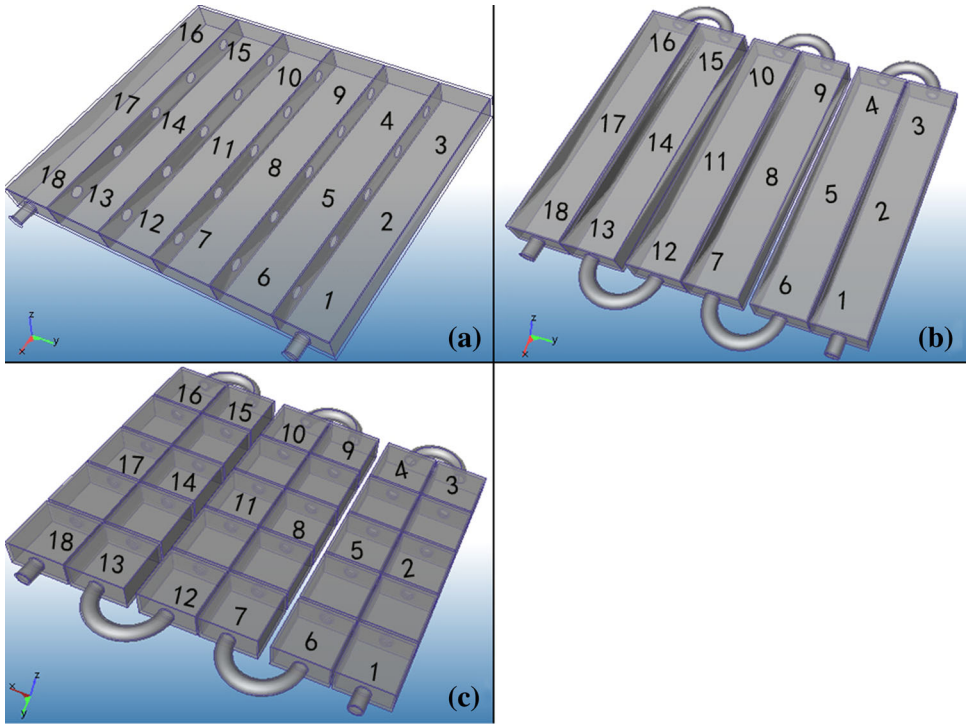

Fig. 3. Three-dimensional model of the plate-shaped (a), stripe-shaped (b), and diamond-shaped (c) TEC.

these TECs, the plate-shaped TEC consisted of two units which can contact with half of the TEMs at one time, as shown in Fig. 3a. The stripe-shaped TEC is made up of six primary units, each of which can attach to five TEMs, as shown in Fig. 3b. The diamond-shaped TEC contains 30 component units, with each unit cooling a thermoelectric module, as shown in Fig. 3c. In addition, 18 points on the TEC are marked for comparison of the experimentally measured and simulated temperatures for further research.

Computational Model

The $k-\varepsilon$ turbulence model was applied in this work. The control equations included the continuity and momentum equations, as shown in Eqs. 2 and 3.

$$\frac{\partial \rho}{\partial t}+\frac{\partial}{\partial x_j}\left(\rho U_j\right)=0, \tag{2}$$

$$\frac{\partial \rho U_i}{\partial t}+\frac{\partial}{\partial x_j}\left(\rho U_i U_j\right)=-\frac{\partial \dot{p}}{\partial x_i} +\frac{\partial}{\partial x_j}\left[\mu_{\text{eff}}\left(\frac{\partial U_i}{\partial x_j}+\frac{\partial U_i}{\partial x_i}\right)\right]+S_{\text{M}}, \tag{3}$$

where S_{M} is the sum of body forces, μ_{eff} is the effective viscosity, and $\dot{p}$ is the pressure. The $k-\varepsilon$ model is based on the eddy viscosity concept, as presented in Eq. 4. Besides, the model assumed that the turbulence viscosity is linked to the turbulence kinetic energy and dissipation via the relation in Eq. 5:

$$\mu_{\text{eff}}=\mu+\mu_{\text{t}}, \tag{4}$$

$$\mu_{\text{t}}=C_\mu \rho \frac{k^2}{\varepsilon}, \tag{5}$$

where μ_{t} is the turbulence viscosity and C_μ is a constant.

Boundary Conditions

Assuming that the exhaust flow in the heat exchanger is fully turbulent and that molecular viscosity can be neglected, the realizable $k-\varepsilon$ turbulence model was adopted, in which the dissipation rate equation can be derived from the dynamic equation of the mean-square vorticity fluctuation at large, turbulent Reynolds number.[6] For processing of the near-wall area with a standard wall function, the heat transfer coefficient and environmental temperature were set as follows.

The temperature of the circulating coolant was approximately 50°C to 80°C when discharged from the radiator. To make full use of the TEM performance, the engine should keep working at high efficiency for high exhaust temperature. At the same time, the TEC must dissipate the heat in time when the vehicle works at high speed, so the coolant inlet temperature was set to 60°C. Based on the operating characteristics of the engine, the inlet

flow rate can reach 8 L/min. The coefficient of heat transfer between the external surface of the heat exchanger and the air was set to 20 W/(m^2 K) with the environmental temperature being set to 30°C.

RESULTS AND DISCUSSION

Validation

To validate the experimental and simulation models, a computational simulation of the TEG system was completed and a bench test was carried out at Wuhan University of Technology to examine its reliability. The experimental system (Fig. 4) consisted of a 2.0-L naturally aspirated engine whose performance parameters are listed in Table I, a dynamometer (maximum power input 160 kW, maximum speed 6000 rpm), and a whole exhaust system. Considering the working performance of the TEG, it is reasonable to install the heat exchanger after the catalytic converter.[7] During the experiment, the exhaust flowed into the heat exchanger to be used as the hot source, while the coolant (engine cooling water) was pumped into the circulating coolant system to form the cold source. The TEMs (Shanghai Institute of Ceramics of the Chinese Academy of Sciences), which were connected electrically in series but thermally in parallel, were divided into two groups arranged on the front and back surfaces of the heat exchanger. Specifically, there were a total of six rows with five modules in each row on both the front and back surface, as shown in Fig. 5. Also, an external fan was applied in the experiment to supply sufficient incoming airflow to simulate the driving condition.

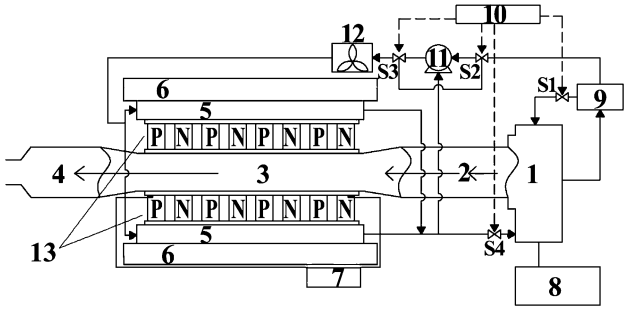

Fig. 4. Schematic of the experimental waste heat recovery system: 1, engine; 2, three-way catalytic converter; 3, heat exchanger for passing exhaust gas; 4, muffler; 5, cooling unit; 6, clamping device; 7, electrical load; 8, dynamometer; 9, radiator; 10, detection controller; 11, SGR pump; 12, axial fan; 13, thermoelectric modules; S1, S2, S3, S4, solenoid switches.

Two different cooling subsystems that can be controlled by solenoid switches (S1, S2, S3, and S4) were included in the experimental system. Several transducers can collect and transform a series of signals, including the coolant temperature, coolant flow rate, and working condition of the engine to the detection controller (10), which controls the solenoid switches. Cooling subsystem A can be seen as part of the engine cooling system with the coolant flowing from the water jacket to the TEC. The other cooling subsystem B is an independent cooling sys-

Table I. Engine performance parameters

Parameter	Value	Parameter	Value
Cylinder number	4	Governed power (kW)	108
Valves per cylinder	4	Governed speed (rpm)	6000
Displacement	1997 mL	Peak torque/speed	200 N m/4000 rpm
Bore/stroke	85 mm/88 mm	Power of pump	0.18 kW
Firing order	1–3–4–2	Cooling mode	Water cooling
Radiator size	547 mm × 415 mm × 50 mm	Number of fan shift	1

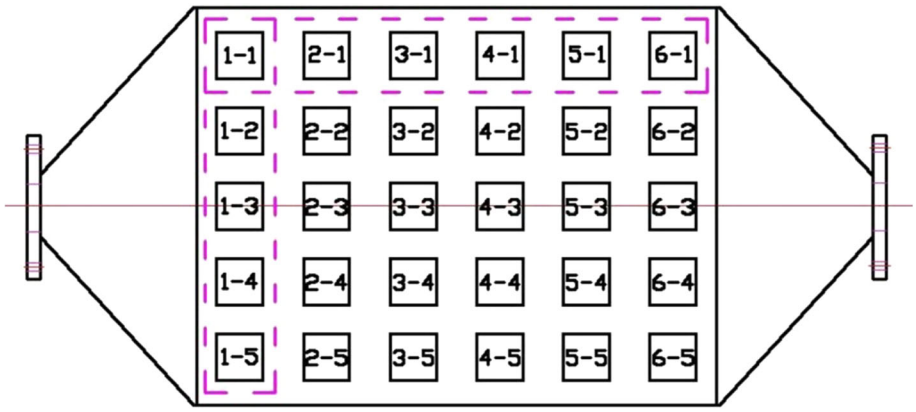

Fig. 5. Module arrangement.

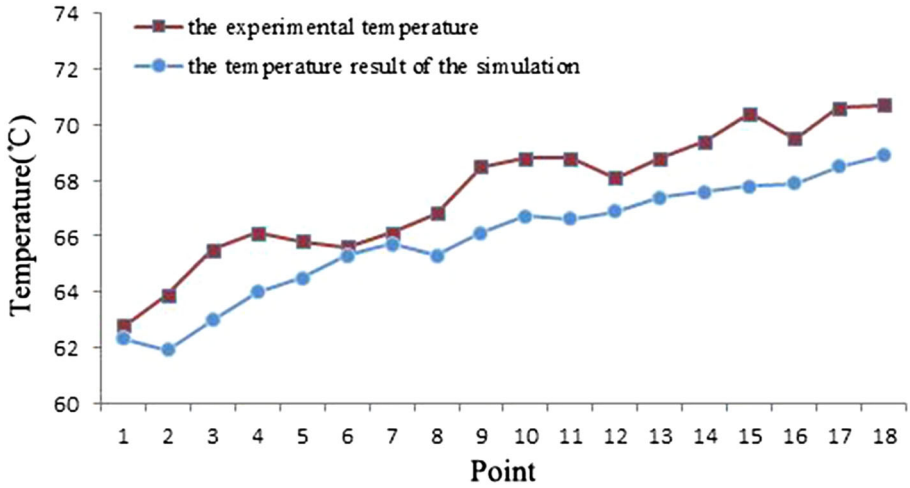

Fig. 6. Temperature comparison of experimental and simulation results.

tem which contains a water pump (11) and an additional radiator with an axial fan (12). Also, a high-power electrical load (7) is connected to the system to measure the voltage and output power.

In the bench test, the exhaust compositions were considered to be invariable for the purpose of analyzing the cooling capability of the different TECs. When the coolant flows out of the TEC, it must be cooled to a certain temperature in order not to affect the heat balance of the engine. The external surface of the TEC was clean and smooth. The experimental conditions including the ambient temperature, ambient winds, modules, clamping force, atmospheric humidity, etc. were kept constant.

The resulting temperatures measured experimentally for the stripe-shaped TEC were compared with the simulation. As presented in Fig. 6, the experimentally measured temperature was slightly higher than the simulated value. Many aspects contribute to this phenomenon; For example, the inlet temperature of the coolant was set to be 60°C in the simulation, while the coolant temperature at the inlet turned out to be about 62°C in the actual working conditions. Also, the ambient temperature in the experiment was about 30°C, possibly showing small fluctuations due to air flow. Besides, the simulation was carried out in an ideal state, while the experiment was not. However, the overall changing trend of the temperature measured in the experiment was basically consistent with the simulation results, confirming the reliability of the experimental and simulation models. Therefore, further simulations and experiments could be meaningfully carried out to obtain more information about the performance of the different TECs.

Discussion of Experimental and Simulation Results for Different TECs

The field synergy principle was adopted to indicate the degree of synergy between the velocity and temperature fields for the entire flow and heat transfer domain; the heat transfer capability is affected by the synergy between the temperature and velocity fields.[8] According to the theory above, the heat transfer can be enhanced by adding turbulence devices to enhance the fluid disturbance and degrade the boundary layer.[9] Based on the thermal energy in the exhaust extracted by the TEMs, a temperature gradient appears on the cold side of the thermoelectric model along the flow direction, and the heat transfer capacity changes in a similar manner.

The simulation results indicate that a sudden expansion appears when the coolant flows through the water inlet into the system, leading to an uneven thermal distribution on the surface of the TEC. Temperature nephograms for the different TECs are presented in Fig. 7. It can be seen that the diamond-shaped TWC (Fig. 7c) exhibits the highest interface temperature, followed by the stripe-shaped TWC (Fig. 7b), and the plate-shaped TWC (Fig. 7a) with the lowest temperature. This result means that the heat of the coolant at the outlet for the diamond-shaped TEC is larger than for the other configurations. Besides, the heat is mainly transferred from the TEMs, and the inlet temperatures for the different TECs are kept the same to ensure that the coolant has the same energy at the inlet. Therefore, in the diamond-shaped TEC, more heat is extracted at the cold side of the TEMs, and the temperature turns out to be the lowest, which is beneficial for constructing a temperature difference between the cold and hot sides of the TEMs.

The coolant trace lines are shown in Fig. 8. From Fig. 8a, it is obvious that two recirculation regions exist, each presenting high temperature, corresponding to the two recirculation regions in the fluid field. By contrast, the stripe-shaped (Fig. 8b) and diamond-shaped TECs (Fig. 8c) do not contain a rotating velocity field, which is adverse to heat convection. In addition, the pressure fields at the symmetrical surface parallel to the hot side of the

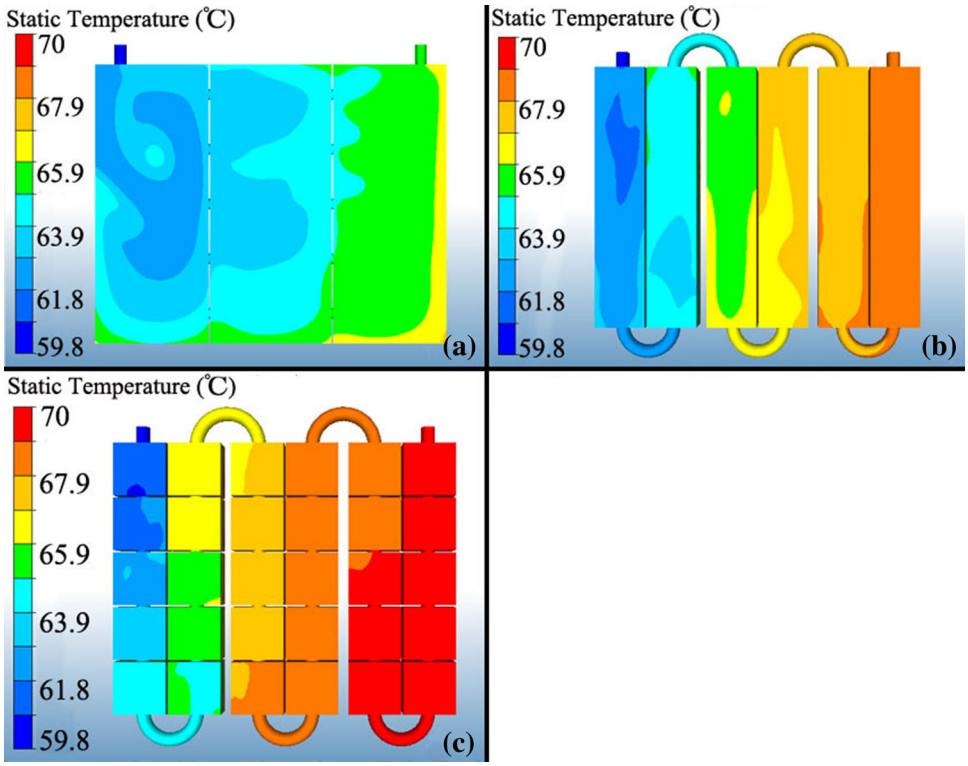

Fig. 7. Temperature field of the plate-shaped (a), stripe-shaped (b), and diamond-shaped (c) TEC.

TEMs are presented in Fig. 9. The coolant is induced to flow through the TEC by the driving force originating from the cylinder jacket cooling pump. The reverse pressure gradient inside the units is observed to balance the driving force and viscous force conspicuously. Because of the TEC, increased pressure is generated to cause the coolant to flow through the unit, which can increase the boiling point of the coolant so that no phase change will occur inside the TEC. As a result, based on the fundamental formula of heat transfer in Eq. 6,

$$\Phi = h \cdot A \cdot \Delta T, \tag{6}$$

expanding the heat transfer area A is an effective way to strengthen the heat convection, which can be realized by fitting baffles to change the internal structure of the conduction surface. According to some numerical calculations, the surface area for the diamond shape is 0.304 m^2, while it is 0.256 m^2 for the stripe shape and 0.166 m^2 for the plate shape. For given heat transfer coefficient h, ambient temperature, and atmospheric humidity, the heat dissipation capacity of the flow will increase and the cold-side temperature of the TEG will reduce for greater heat transfer area A and higher surface temperature. Based on this analysis, the cooling capability of the diamond-shaped TEC is considerable.

Additionally, experiments need to be carried out to verify the simulation results for the different TECs. According to the previous results, a slight discrepancy in temperature differences can be neglected, so that the baseline for the comparison is fixed. The changing trends for the temperature on the different TECs are presented in Fig. 10, showing that the temperatures of the diamond-shaped and stripe-shaped TECs are much higher than that of the plate-shaped TEC. Although the temperature of the diamond-shaped TEC is not always the highest, the most important feature is that the outlet temperature of the diamond-shaped TEC is higher than that of the other two TECs, which is in full compliance with the simulation results.

Finally, the measured curves of output power for different engine speeds are shown in Fig. 11, which presents the maximum output power measured by an electrical load at matching load conditions. From analysis of the engine operating characteristics, it can be concluded that the exhaust temperature at the inlet rises uniformly with increasing engine speed,[10] which will lead to growth of the output power. As these results show, compared with the TEG with the stripe-shaped or plate-striped TECs, the TEG with diamond-shaped TEC can convert more heat into electrical energy to improve the efficiency of the whole system. Except for the plate-shaped TEC, the power difference between the diamond-shaped and stripe-shaped TWCs increases as the engine speed rises from 2700 r/min to 3000 r/min. Conversely, this power difference decreases when the speed increases further. To summarize,

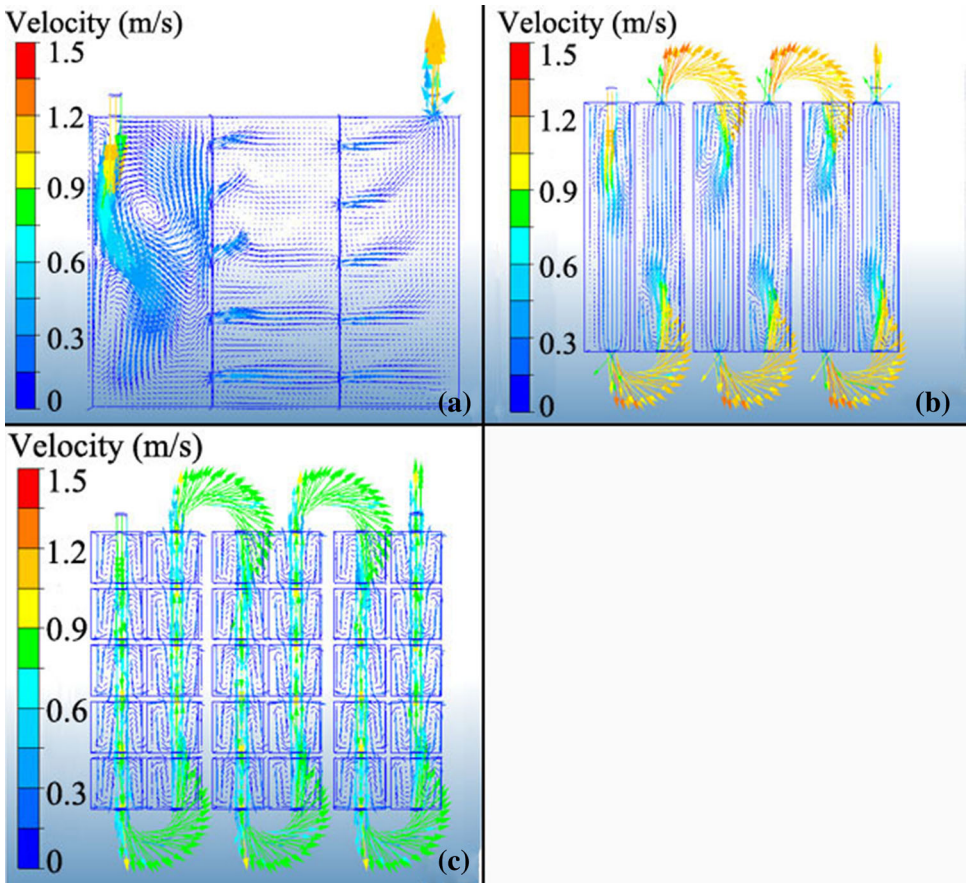

Fig. 8. Velocity field of the plate-shaped (a), stripe-shaped (b), and diamond-shaped (c) TEC.

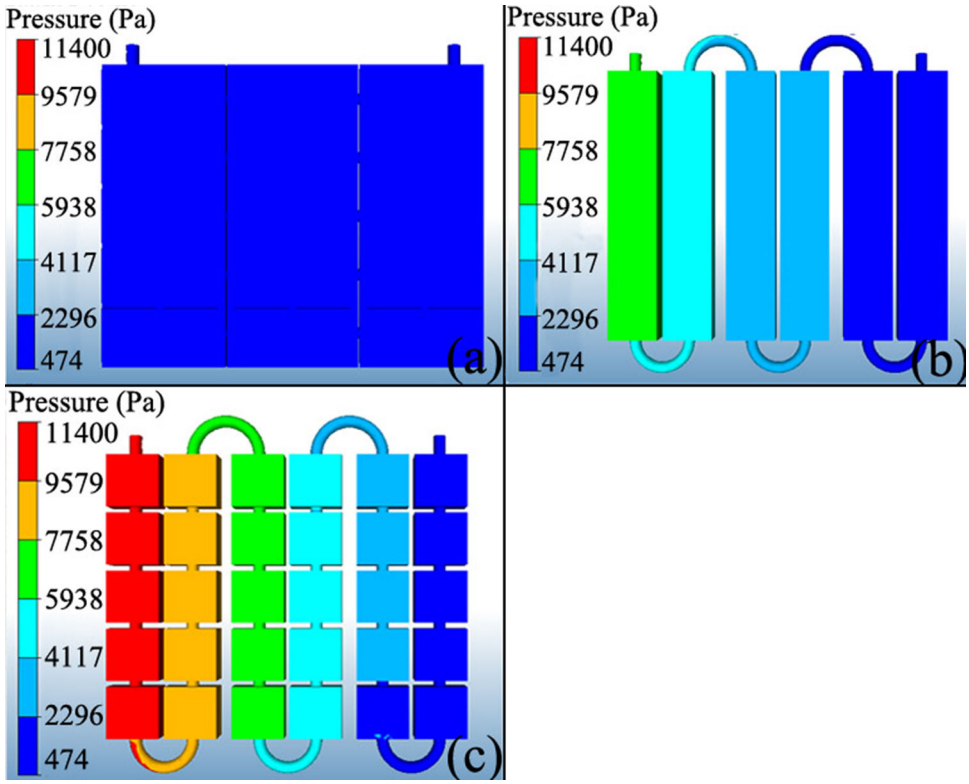

Fig. 9. Pressure field of the plate-shaped (a), stripe-shaped (b), and diamond-shaped (c) TEC.

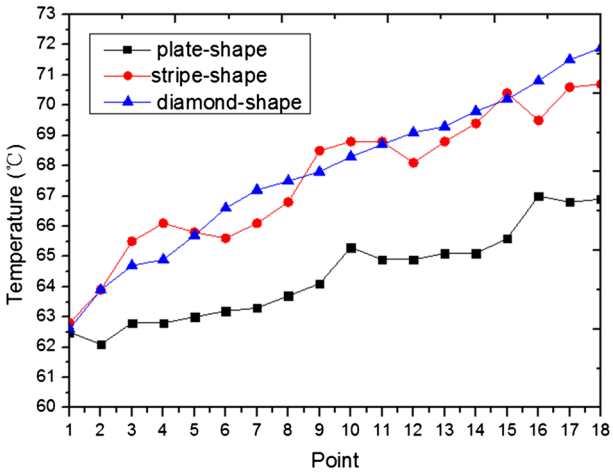

Fig. 10. Variation of experimental temperature for the different TECs.

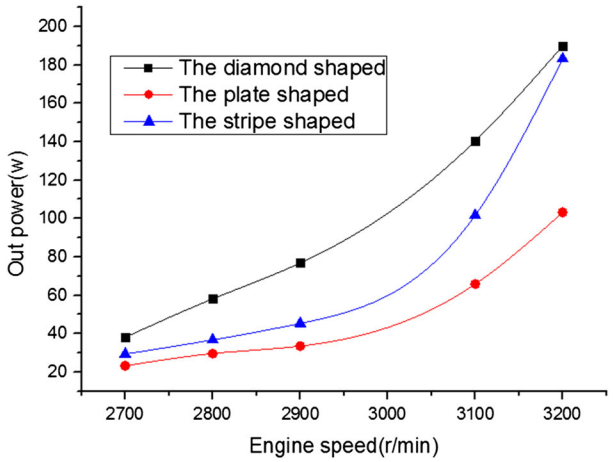

Fig. 11. Variation of experimental output power with engine speed.

when the engine speed exceeds a certain value, the thermoelectric power production becomes less sensitive to the TEC configuration, because the exhaust temperature becomes so high that the limited cooling capability of the TEC cannot transfer the heat in time.

CONCLUSIONS

In this work, three different configurations of TECs and the whole TEG system for recovering waste heat from automotive exhaust were proposed and analyzed. The simulation results provide accurate details of the temperature distribution on the different TECs, which can improve the accuracy of analytical results. According to the consistency between the experimental and simulation results, the diamond-shaped TEC made of aluminum alloy and with surface area of 0.304 m^2 represents the ideal choice for the cold side of the TEG system. It can reduce the thermal resistance (between the TEC and the TEMs) and transfer more heat to ensure that the cold side of the TEMs stays at low temperature.

The current study focused on structural optimization of the TEC to improve the TEG efficiency. In future study, the method based on simulation modeling with experimental verification introduced herein must be combined with heat transfer theory to enable further structural design and optimization to improve the overall exhaust heat utilization and enhance the power generation.

ACKNOWLEDGEMENTS

This work was funded by Grant No. 2013CB632505 from the National Basic Research Program of China (973 Program) and supported by the Fundamental Research Funds for the Central Universities (WUT 142207005).

REFERENCES

1. J. Yang and F.R. Stabler, *J. Electron. Mater.* 38, 1245 (2009).
2. Y.Y. Hsiao and W.C. Chang, *Energy* 35, 1447 (2010).
3. A. Rezania and L.A. Rosendahl, *Int. Commun. Heat Mass Transf.* 39, 1054 (2012).
4. Y.D. Deng, X. Liu, and S. Chen, *J. Electron. Mater.* 43 (2014) (in press).
5. D.M. Rowe and G. Min, *J. Power Sources* 73, 193 (1998).
6. T.H. Shih and W.W. Liou, *Comput. Fluids* 24, 227 (1995).
7. C.Q. Su and N.Q. Tong, *J. Electron. Mater.* 42, 1877 (2013).
8. Z.Y. Guo and W.Q. Tao, *Int. J. Heat Mass Transf.* 48, 1797 (2005).
9. S.M. Yang, *Heat Transfer Theory* (Beijing: Higher Education, 2004), p. 207.
10. Y.C. Wang and C.S. Dai, *Appl. Energy* 112, 1171 (2013).